Eliminating the effect of acoustic noise on cantilever spring constant calibration

Cite as: Appl. Phys. Lett. **113**, 233105 (2018); https://doi.org/10.1063/1.5063992
Submitted: 03 October 2018 . Accepted: 19 November 2018 . Published Online: 07 December 2018

Aaron Mascaro, Yoichi Miyahara, Omur E. Dagdeviren, and Peter Grütter

Eliminating the effect of acoustic noise on cantilever spring constant calibration

Aaron Mascaro,[a] Yoichi Miyahara, Omur E. Dagdeviren, and Peter Grütter
Department of Physics, McGill University, 3600 Rue University, Montreal, Québec H3A2T8, Canada

(Received 3 October 2018; accepted 19 November 2018; published online 7 December 2018)

A common use of atomic force microscopy is quantifying local forces through tip-sample interactions between the probe tip and a sample surface. The accuracy of these measurements depends on the accuracy to which the cantilever spring constant is known. Recent work has demonstrated that the measured spring constant of a cantilever can vary up to a factor of five, even for the exact same cantilever measured by different users on different microscopes. Here, we demonstrate that a standard method for calibrating the spring constant (using oscillations due to thermal energy) is susceptible to ambient acoustic noise, which can alter the result significantly. We demonstrate a step-by-step method to measure the spring constant by actively driving the cantilever to measure the resonance frequency and the quality factor, giving results that are unaffected by acoustic noise. Our method can be performed rapidly on any atomic force microscope without any expensive additional hardware. *Published by AIP Publishing.* https://doi.org/10.1063/1.5063992

Atomic force microscopes (AFMs) have become an invaluable tool across many areas of materials science research due to their ability to probe the structural and electrical properties of materials with extremely high spatial resolution. Modern AFMs rely on a micro-fabricated sharp probe tip protruding from the end of a cantilever beam to sense exceptionally small forces.[1–5] In many experiments, the interaction force itself is to be measured, which is generally done by measuring the change in the mechanical status of the cantilever (static deflection, oscillation amplitude, or change in the resonance frequency) as it interacts with the surface.[4,6–9] Independent of the operation mode of the AFM, the spring constant of the cantilever needs to be known to convert the measured cantilever response to units of force, which can then be used to quantify the tip-sample interaction strength.[3,10–12]

There are several methods currently used to quantify spring constants including the method of Cleveland *et al.*,[13] where the cantilever's resonance frequency (ω_0) is measured before and after adding known masses to the end of the cantilever, and Sader's method,[14] which requires knowledge of the cantilever's resonance frequency (ω_0), quality factor (Q), plan-view dimensions (length L and width b), and the viscous medium the cantilever resides in (typically air). Due to its non-invasive nature, Sader's method has been widely adopted across commercial AFM systems for cantilever spring constant calibration. A common implementation of Sader's method is to measure the power spectral density (PSD) of the cantilever's deflection to observe the thermal oscillations, which can then be used to extract both the quality factor and the resonance frequency, although Sader's method is fundamentally agnostic as to how the quality factor and the resonance frequency are actually measured. Sader *et al.* have recently shown that the variation of these parameters obtained by fitting the measured thermal PSD can lead to differences of up to a factor of 5 in the spring constant obtained using Sader's method by different users on different microscopes even for the exact same cantilever, while a previous study by te Reit *et al.* demonstrated variations of up to a factor of 2.[15,16] This technique assumes that thermal fluctuations are the sole driving force acting on the cantilever, which results in spectrally white multiplicative noise.[17] This may be true in many cases; however, we demonstrate that additional noise sources such as ambient acoustic noise can cause the overall driving force to deviate from white Gaussian noise, which can alter the values obtained by fitting the measured PSD to that of a damped driven harmonic oscillator driven by Brownian noise. Furthermore, we demonstrate that by actively driving the cantilever, we can obtain reliable measurements of the resonance frequency and the quality factor that are impervious to increased ambient acoustic noise levels.

Figures 1(a) and 1(c) show the typical frequency spectra of thermal oscillation peaks of two different cantilevers (Type 1: OPUS 4XC-NN-A and Type 2: OPUS 4XC-NN-B) obtained by recording the AFM deflection signal at a sample rate of 2.5 MHz for 2.5 s, taking a fast-Fourier transform (FFT), and then averaging it 50 times (similar to the procedure in Ref. 18). Modelling the cantilevers as damped driven harmonic oscillators, the frequency spectra of the oscillation peaks are given by

$$F(\omega, \bar{\alpha}) = \frac{\alpha_1/\omega_0^2}{(1-(\omega/\omega_0)^2)^2 + (\omega/\omega_0 Q)^2} + \alpha_2, \qquad (1)$$

where $F(\omega, \bar{\alpha})$ is the power spectral density (PSD) (in V^2/Hz or m^2/Hz), α_1 is the amplitude, and α_2 is the baseline noise level. A least-squares fit to the logarithm of Eq. (1) is shown as the solid black line in each panel of Fig. 1, where the window sizes are large compared to the spectral width of the Lorentzians (corresponding to a normalized window size of $\beta \approx 17$, as defined by Sader *et al.*[19]) which results in small uncertainties on the fit parameters. Since the thermal noise is multiplicative, taking the logarithm of both sides of Eq. (1) removes the weighting of the squared errors in the least-squares minimization procedure and results in residuals that are zero-centered. Fitting the PSD data directly (without

[a]Electronic mail: mascaroa@physics.mcgill.ca

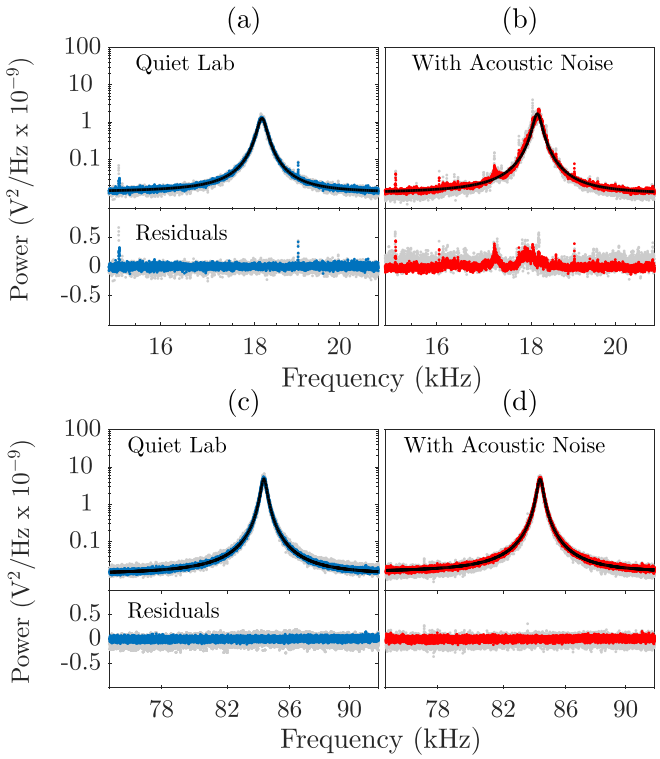

FIG. 1. Measured PSD around the cantilever resonance for cantilever 1-A: (a) without acoustic noise and (b) with ambient acoustic noise and cantilever 2-A: (c) without acoustic noise and (d) with ambient acoustic noise. Coloured data are the average of 5 independent measurements of 50 spectra averaged together, while the grey data show one such measurement of 50 spectra averaged. Black lines are the fits to the logarithm of Eq. (1).

taking the logarithm) decreases the effect of the off-resonance background noise, but is still significantly influenced by noise in the resonance peak (see supplementary material, Fig. S4).

To study the effect of ambient noise on the measurements, a speaker (Motorola J03 type) was connected to the output of a function generator (Agilent 33220a) outputting white noise with a bandwidth of 9 MHz and placed near the AFM. A similar experiment was conducted by Koralek *et al.*, in which an AFM cantilever was driven by applying a white noise signal to the drive piezo in the cantilever holder allowing them to emulate thermal oscillations of the cantilever at much higher temperatures than physically accessible.[20] In our case, the noise source is only coupled to the cantilever via air and thus simulates the effect of increased ambient acoustic noise. The frequency spectra of cantilevers 1-A and 2-A with ambient acoustic noise are shown in Figs. 1(b) and 1(d). To preclude the effects of slowly changing extrinsic variables that could affect the measurements, the quiet and noisy measurements were done in an alternating fashion.

Equation (1) was used to determine the quality factor, the resonance frequency, the baseline noise level, and the amplitude of four different cantilevers, two of Type 1 with resonance frequencies in the audio range (~20 kHz) and two of Type 2 with resonance frequencies well into the ultrasonic range (~80 kHz). These results are shown in Figs. 2(b) and 2(c), where the error bars are the standard deviation of the mean for 5 independent measurements of each cantilever. The shaded regions are the theoretical uncertainties for the fit parameters calculated using the formulas in Refs. 19 and 18 (see supplementary material). The "noisy" data (red data points in Fig. 2) are values obtained from fitting the frequency spectra with ambient acoustic noise as described.

The spring constant for a rectangular cantilever can be directly calculated as

$$k_n = 0.1906\rho b^2 L Q\,\Gamma_i(\omega_0)\omega_0^2, \tag{2}$$

where the prefactor (0.1906) comes from the normalized effective mass and Γ_i is the imaginary component of the hydrodynamic function.[14] The spring constants for all four cantilevers were calculated using Eq. (2), and are shown in Fig. 2(a).

To study the systematic effect of the acoustic noise level on the fit parameters, PSDs were also taken with increasing acoustic noise and the spring constants obtained from the fit parameters (Q and f0) were examined (see supplementary material). The result shown in Fig. 3 demonstrates a clear systematic change in the measured spring constant with increasing acoustic noise (shown for cantilever 1-A).

Another method of measuring the resonance frequency is to drive the cantilever using a sine wave and sweeping its frequency. This can be done using a piezo-acoustic drive, which is susceptible to the non-flat transfer function of the system.[21] Since the quality factor is equal to f_0/FWHM (where f_0 is the resonance frequency in Hz and FWHM is the

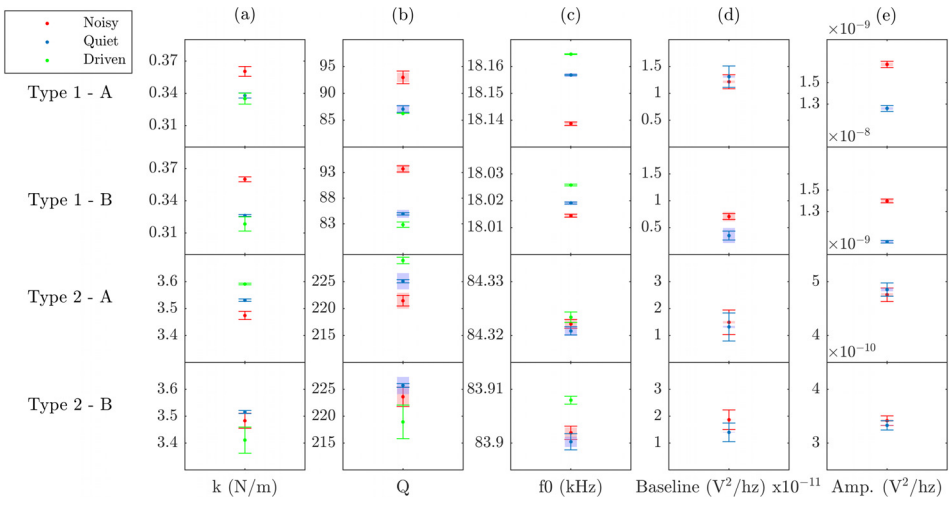

FIG. 2. (a) Spring constants obtained from Eq. (2), (b) quality factors, (c) resonance frequencies ($\omega_0/2\pi$), (d) baseline noise levels (α_2) and (e) peak amplitudes (α_1) obtained from fitting the "thermal" oscillation PSD measurements of 4 different cantilevers with (red) and without (blue) ambient acoustic noise to Eq. (1). The results of the driven-calibration method described in the text are shown in green. Error bars are the uncertainty on the mean from 5 measurements on each cantilever. Shaded regions are theoretical uncertainties on the fit parameters calculated using the formulas given in Refs. 19 and 18.

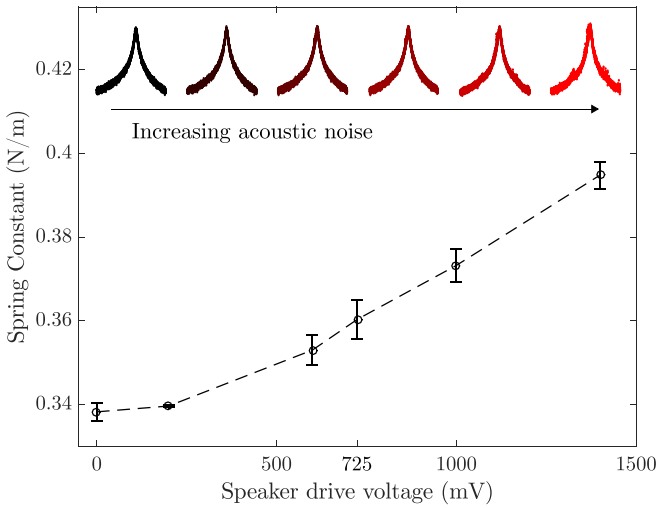

FIG. 3. Spring constant obtained from thermal PSDs for cantilever 1-A as a function of white noise drive voltage sent to the speaker. Inset plots show the raw spectra for each of the 6 data points.

full width at half-maximum of the resonance peak) and typical quality factors are ∼200 for the ∼80 kHz cantilevers used in this experiment, the frequency span required to measure Q from a driven spectrum would be at least 1 kHz. Thus, determining Q from a driven cantilever response by fitting the peak would be highly susceptible to transfer function irregularities and/or spurious resonances within this ∼1 kHz range. We can, however, measure the resonance frequency of the cantilever very accurately by sweeping over a small frequency window and fitting the response to Eq. (1) as the transfer function should have a minimal impact as long as the frequency span is small enough (see supplementary material, Figs. S1 and S2). Multiple measurements on cantilever Type 2-A are shown in Fig. 4(a) along with their fitted curves (black lines). The inset shows the accuracy of the fits; each measurement is within 2 Hz of the mean and the uncertainty on the mean is under 1 Hz. The measurement is unaffected by adding acoustic noise (i.e., the results with and without noise are the same), which is expected because the additional acoustic energy being added to the system is orders of magnitude smaller than the kinetic energy of the driven cantilever.

To measure the quality factor using a driven technique, we can simply record the ringdown time. This was performed by driving the cantilevers at the resonance frequency previously measured and suddenly turning off the driving force. By directly recording the AFM deflection signal, we can observe the oscillation amplitude decreasing, as shown in Fig. 4(b). The peak values can be easily extracted using a peak-finding algorithm, and they decrease exponentially over time, which is given by

$$y = Ae^{-t/\tau}, \tag{3}$$

where τ is the decay time constant and A is the exponential prefactor. The quality factor is related to the decay time constant by

$$Q = \tau f_0 \pi. \tag{4}$$

In fitting the peak amplitudes to Eq. (3), one has to be aware of the effect of the non-zero noise floor of the

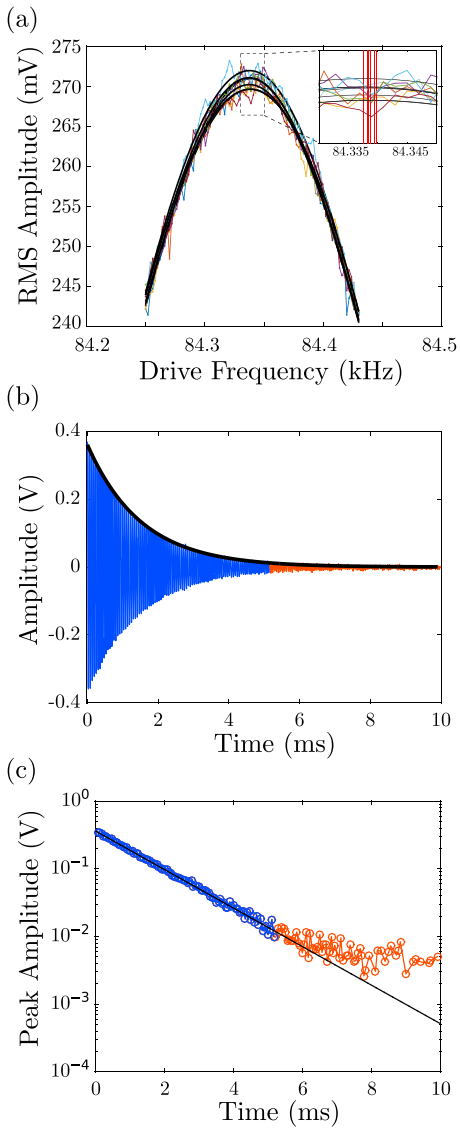

FIG. 4. (a) Driven response amplitude (RMS) of cantilever 1-A across the resonance frequency showing curves fitted to Eq. (1). Inset shows a closeup, where the red vertical lines mark the resonance frequency obtained from each fitted curve. (b) AFM deflection signal directly after turning off the driving force (at t = 0) along with the fit to Eq. (3) for multiple measurements on cantilever Type 1-A. (c) Driven response amplitude (RMS) of cantilever Type 1-A across the resonance frequency showing curves fitted to Eq. (3). Inset in (a) shows a closeup where the red vertical lines mark the resonance frequency obtained from each fitted curve.

measurement device. This becomes apparent when plotted on a log scale: as the peak values approach the noise floor, they begin to deviate from the expected straight-line behaviour, as shown by the orange data points in Fig. 4(c). This can easily be corrected for by simply measuring the noise-floor, which we define as the peak-to-peak noise on the deflection signal with the drive being turned off, and then only including peak values greater than this value in the fit. These are shown in blue in Fig. 4(c), while the red data points were not included in the fit.

Measuring the ringdown with the initial drive frequency slightly off resonance was also investigated to determine how accurately the resonance frequency must be measured initially. There were no significant deviations in the measured quality factor with the drive frequency within approximately

± 10 Hz of resonance, thus demonstrating the robustness of this technique (see supplementary material, Fig. S3).

The results of each cantilever from the sweep and ringdown measurements are shown in green in Fig. 2. The same values were obtained with and without ambient acoustic noise.

Although we used the ringdown method for quality factor measurements, there exist other driven techniques to extract the quality factor as well, including by taking the derivative of the measured phase vs. frequency data. This quantity is related to the quality factor by $\frac{d\phi}{d\omega}|_{\omega=\omega_0} = 2Q/\omega_0$, where ϕ is the oscillator phase with respect to the drive signal.[22] The main drawback of this technique is the numerical derivative that must be computed, which is widely known to greatly amplify the noise present in the data. This technique therefore requires significant averaging in order to obtain reliable results, and in addition, it is also susceptible to transfer function irregularities as with any measurement where the drive frequency is swept. The ringdown technique, on the other hand, requires excitation at a single frequency and is thus impervious to effects related to the mechanical transfer function.

As can be observed in Fig. 1, ambient acoustic noise can affect the measured PSD. This is immediately apparent in the case of the audio-frequency range cantilever Type 1-A [Figs. 1(a) and 1(b)], while the spectrum of the ultrasonic frequency-range cantilever Type 2-A is visually indistinguishable with and without ambient acoustic noise [Figs. 1(c) and 1(d)]. As shown in Fig. 2(a), the spring constant obtained from fitting the thermal PSD may be systematically overestimated by 10% in some cases (Type 1 cantilevers), while in others it may be underestimated (Type 2-A), and in the best case there is no observed difference (Type 2-B). Using the driven techniques we described, however, yielded spring constants that were consistent with those obtained from the quiet thermal spectral measurements and unaffected by acoustic noise.

Type 2 cantilevers have both larger spring constants and resonance frequencies in the ultrasonic range. The acoustic noise generated by the speaker does extend well into the ultrasound; however, atmospheric attenuation at higher frequencies is known to be severe.[23] Thus, as expected, the stiffer, higher frequency cantilevers are less affected by ambient acoustic noise, but not impervious to it. To understand why the fit results differ for cantilever 2-A even though there are no clear visual differences in the data, it is instructive to look at the variance of the residuals (R) since the residuals are proportional to the logarithm of the noise. Taking $\mathrm{Var}[10^R]$, where $R = \log_{10}[y] - \log_{10}[F(\omega, \bar{\alpha})]$ [i.e., the logarithm of the data minus the logarithm of the fit function, Eq. (1), which gives a unitless quantity], we can compare how "noisy" the residuals are. For cantilever 1-A, the variances are: $3.0 \pm 0.3 \times 10^{-2}$ for the quiet data and $5.8 \pm 0.4 \times 10^{-2}$ for the noisy data, while for cantilever 2-A, the variances are: $2.06 \pm 0.04 \times 10^{-2}$ for the quiet data and $2.42 \pm 0.04 \times 10^{-2}$ for the noisy data. In both cases, the residuals are significantly noisier when the acoustic noise is on.

This discrepancy is fundamentally due to the fact that the observed spectrum is not always thermally limited; there can be contributions from various sources of detection noise (e.g., optical shot noise), electronic noise, and mechanical vibrations (e.g., acoustic noise from vacuum pumps). The former have been investigated comprehensively for optical beam deflection systems such as the one used here,[24–28] while the effect of mechanical vibrations on the thermal oscillations of tuning forks has been discussed in brief.[29] Since the energy of the thermal oscillations is so small, even a small amount of mechanical noise (acoustic or otherwise) can have a non-negligible effect and lead to deviations from a spectrally white driving force. This is evident in the residuals plotted in Fig. 1(b). The deviation from a Lorentzian is due to the acoustic energy being converted into mechanical oscillations of the cantilever around the cantilever's resonance frequency. Note that the mechanical transfer function of an AFM system is not flat in frequency due to many unavoidable non-linear mechanical couplings existing between the different microscope components. It is these couplings that lead to frequency dependent phase shifts described and measured in Ref. 21. The exact mechanism by which acoustic noise presents in the cantilever deflection PSD is expected to be highly dependent on the geometry of the microscope and the noise source itself. By actively driving the cantilevers, however, the energy of the mechanical oscillations can be increased well above the noise floor making them insensitive to ambient acoustic noise.

As we have shown, ambient acoustic noise can introduce systematic errors into thermal measurements of cantilever quality factors, which can propagate to errors in calculated spring constants. This effect is especially pronounced for cantilevers with resonance frequencies in the audio range ($<$20 kHz), but can also be present for cantilevers with resonance frequencies well above this. By actively driving the cantilever to measure the resonance frequency and the quality factor, the effect of acoustic noise can be mitigated. The quality factor can reliably be measured by recording the ringdown directly and fitting this to a decaying exponential. The fit should be done such that data above the noise floor only are included. This procedure results in highly reproducible measurements that can be used to calculate the spring constant of a cantilever using standard techniques. It also precludes systematic errors due to ambient acoustic noise, which may contribute to the observed differences in cantilever spring constants obtained on different atomic force microscopes and/or by different users.

See supplementary material for the transfer function effects, the effect of drive frequency on ringdown, the results of fitting PSDs directly, and the effects of acoustic noise on f_0 and Q.

The authors acknowledge financial support from the Natural Sciences and Engineering Research Council of Canada and the Fonds de recherche du Quebec-Nature et Technologies.

[1]T. Albrecht, S. Akamine, T. Carver, and C. Quate, J. Vac. Sci. Technol. A: Vac., Surf., Films **8**, 3386 (1990).
[2]F. Ohnesorge and G. Binnig, Science **260**, 1451 (1993).
[3]H.-J. Butt, B. Cappella, and M. Kappl, Surf. Sci. Rep. **59**, 1 (2005).
[4]R. Raiteri, M. Grattarola, H.-J. Butt, and P. Skládal, Sens. Actuators B: Chem. **79**, 115 (2001).
[5]F. J. Giessibl, Science **267**, 68 (1995).

[6]M. Li, H. X. Tang, and M. L. Roukes, Nat. Nanotechnol. **2**, 114 (2007).
[7]A. Noy, D. V. Vezenov, and C. M. Lieber, Annu. Rev. Mater. Sci. **27**, 381 (1997).
[8]P. A. Wiggins, T. Van Der Heijden, F. Moreno-Herrero, A. Spakowitz, R. Phillips, J. Widom, C. Dekker, and P. C. Nelson, Nat. Nanotechnol. **1**, 137 (2006).
[9]N. Balke, P. Maksymovych, S. Jesse, I. I. Kravchenko, Q. Li, and S. V. Kalinin, ACS Nano **8**, 10229 (2014).
[10]F. J. Giessibl, Appl. Phys. Lett. **78**, 123 (2001).
[11]J. E. Sader and S. P. Jarvis, Appl. Phys. Lett. **84**, 1801 (2004).
[12]R. García and R. Perez, Surf. Sci. Rep. **47**, 197 (2002).
[13]J. Cleveland, S. Manne, D. Bocek, and P. Hansma, Rev. Sci. Instrum. **64**, 403 (1993).
[14]J. E. Sader, J. W. Chon, and P. Mulvaney, Rev. Sci. Instrum. **70**, 3967 (1999).
[15]J. E. Sader, R. Borgani, C. T. Gibson, D. B. Haviland, M. J. Higgins, J. I. Kilpatrick, J. Lu, P. Mulvaney, C. J. Shearer, A. D. Slattery *et al.*, Rev. Sci. Instrum. **87**, 093711 (2016).
[16]J. Te Riet, A. J. Katan, C. Rankl, S. W. Stahl, A. M. van Buul, I. Y. Phang, A. Gomez-Casado, P. Schön, J. W. Gerritsen, A. Cambi *et al.*, Ultramicroscopy **111**, 1659 (2011).
[17]L. D. Landau and E. M. Lifshitz, *Course of Theoretical Physics* (Elsevier, 2013).
[18]J. E. Sader, B. D. Hughes, J. A. Sanelli, and E. J. Bieske, Rev. Sci. Instrum. **83**, 055106 (2012).
[19]J. E. Sader, M. Yousefi, and J. R. Friend, Rev. Sci. Instrum. **85**, 025104 (2014).
[20]D. Koralek, W. Heinz, M. Antonik, A. Baik, and J. Hoh, Appl. Phys. Lett. **76**, 2952 (2000).
[21]A. Labuda, Y. Miyahara, L. Cockins, and P. H. Grütter, Phys. Rev. B **84**, 125433 (2011).
[22]J. B. Marion, *Classical Dynamics of Particles and Systems* (Academic Press, 2013).
[23]B. D. Lawrence and J. A. Simmons, J. Acoust. Soc. Am. **71**, 585 (1982).
[24]H.-J. Butt and M. Jaschke, Nanotechnology **6**, 1 (1995).
[25]T. Fukuma, Rev. Sci. Instrum. **80**, 023707 (2009).
[26]F. J. Giessibl, H. Bielefeldt, S. Hembacher, and J. Mannhart, Appl. Surf. Sci. **140**, 352 (1999).
[27]A. Labuda, J. R. Bates, and P. H. Grütter, Nanotechnology **23**, 025503 (2012).
[28]F. Gittes and C. F. Schmidt, Eur. Biophys. J. **27**, 75 (1998).
[29]J. Welker, F. de Faria Elsner, and F. J. Giessibl, Appl. Phys. Lett. **99**, 084102 (2011).